Journal of Energy and Safety Technology

JEST

RESEARCH ARTICLE Open Access

Monitoring and Visualization of Solar PV Thermal Flow via Interpolation Techniques

Feras A. Hafiz[1], Y.I. Go[1*], Rodney H.G. Tan[2], Saqaff A. Alkaff[1], T.H Tan[2], T.C. Yap[1]

[1]School of Engineering and Physical Sciences, Heriot-Watt University, 62200 Putrajaya, Malaysia
[2]Faculty of Engineering, Technology & Built Environment, UCSI University, 56000 K.L., Malaysia
Corresponding author: y.go@hw.ac.uk

Article History

Received: March 15, 2018 Received in revised form: Oct 31, 2018 Accepted: Nov 12, 2018 Published: Nov 30, 2018

Abstract

Temperature is one of the major factors that affect the efficient of solar panels and temperature profiles on solar panel are required to optimise the performance of solar PV. A method to construct and visualise the thermal profiles of solar panel with minimum temperature measurement is proposed in this work. Based on nine measured temperature, three different interpolation techniques are used to predict the temperature at 25 points and 81 points. The predicted temperature is then compared with measured temperature from thermal gun. MATLAB is used to reconstruct the thermal image in two different resolution, 17x17 and 33x33. Bilinear interpolation technique and resolution of 33x33 gives the best results and can be applied in industry to predict temperature profile on solar panel with minimum measurement.

Keywords: Bilinear; cubic spline; nearest; temperature profile

1.0 INTRODUCTION

The commercial solar panels have efficiency ranged from 15-25% [1]. The efficiency of solar photovoltaic panel relies on many factors such as ambient temperature, wind direction, solar radiation and others. Most researchers agree that changes in solar radiation or temperature on a solar panel have a major impact on the output power generated by a solar panel, understand the relationship will help engineers and researchers to improve or optimize the power production of solar panel [2, 3]. Temperature profile and its progression in a solar PV system are very important to know because this information allows users to correlate the relationship between the power output and the thermal flow in a PV system and then optimise the system. However, the presence of thermal flow or temperature profile of solar module is impossible to visualise with bare eyes. This project intends to generate the thermal profile of solar PV system through minimum temperature measurement (nine measurement). Three interpolation methods will be used to calculate the temperature data of more strategy locations on the PV panel. The temperature profile is then reconstructed with MATLAB and presented in two resolutions.

2.0 LITERATURE REVIEW

The output of a PV module is affected by different parameters, one of the major parameters is temperature. Fig. 1 shows the I-V characteristics curve of a solar module at four different temperatures. In general PV modules perform better at lower temperature. It is difficult to study the effect of solar radiation on PV modules due to the influence of different factors on the sunlight spectrum such as difference in temperatures on the solar disc and atmosphere influence [4]. Determining the maximum power point (MPP) of solar photovoltaic system helps to optimise the performance of the system.

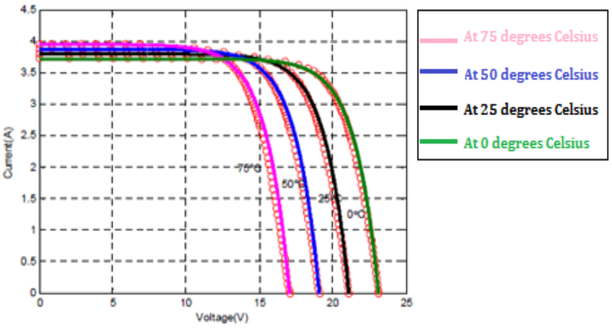

Fig. 1 PV module I-V curve characteristics under different temperatures [5].

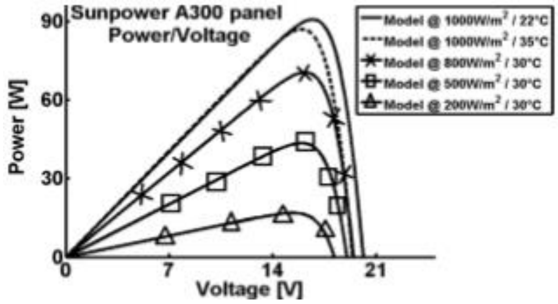

Fig. 2 Maximum power tracking result sample [6].

2.1 Maximum Point of Tracking Method with Parabolic Interpolation

Solar cell converts sunlight into electrical energy; however; most of the solar radiation lost in the form of heat when reaching the earth surface. Thus, it has become a major interest of many researchers to track the maximum thermal and power point of a solar cell in the PV system due to non-linear of current and voltage characteristics resulting from fluctuation in the ambient temperature of the solar module and intensity of sunlight. Hence, operating a PV system at the MPP will allow supplying the maximum power to the load even in unstable weather conditions. In order to understand and to determine the maximum power output that results to a maximum thermal point of a PV cell, strategy proposed is to use a current sensing device that could sense the output current of the system on a timely basis, therefore power generated from the system is resulting from a change in temperature (T), irradiance (E), and other parameters can be determined by MPP alone using parabolic interpolation method, though this requires much of iteration [6]. Fig 2 shows the sample of maximum power tracking results.

2.2 Data Measurement and Monitoring Techniques

Modelling the characteristics of a thermal flow for a PV module is affected by fluctuation of irradiance. The relationship of temperature with irradiance was studied by Jones and Underwoord, as shown in Fig 3. An exponential decay in irradiance is noticed when the temperature dropped over a short period of time [7]. This indicates a significant relationship in temperature and irradiance. Fig. 4 shows a visualization of the thermal flow for multiple modules in a solar array. The temperature profile was predicted based on measured temperature through multiple thermocouples sensors attached at the rear surface of PV panels in the array [8]. Non-linear optimisation method is used for forecast the data of non-measured area. However, accuracy of the predicted value depends on a chosen algorithm, the initial condition of the model and the objective of the modelling [9]. Different optimization methods would be considered, these methods are particle swarm optimization, bacteria foraging algorithm, simulated annealing harmony search, cuckoo search, pattern searching optimization, & bird mating optimizer [10].

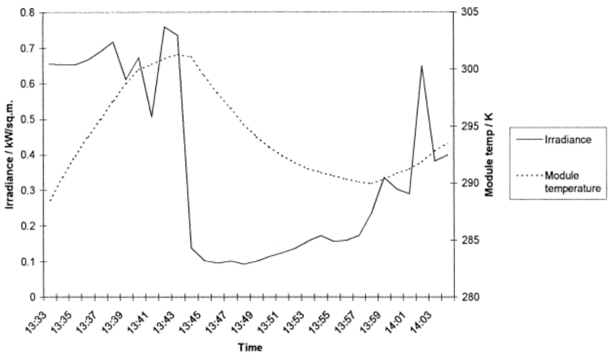

Fig. 3 Changes observed in temperature with respect to irradiance change [7].

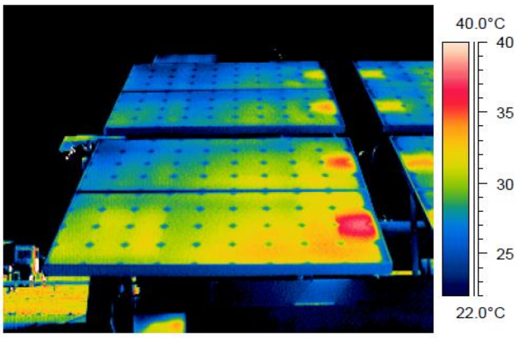

Fig. 4 Thermal flow visualization of multiple modules in a solar array [8].

3.0 METHODOLOGY

The attempt to monitor and visualise solar PV thermal flow consists of several stages, as presented in Figure 5. The temperature of selected locations on solar module were first measured with 9 NTC thermistor temperature sensors. The temperature data were then processed by microcontroller and sent to computer. Based on the nine measured points, the temperature at various location is predicted using three interpolation techniques with MATLAB software. Thermal image is then reconstructed based on the interpolated temperature values. The interpolated temperature is verified with the more measured temperature with infrared thermogun. Detailed methodology is reported by Mangeni et. al [11].

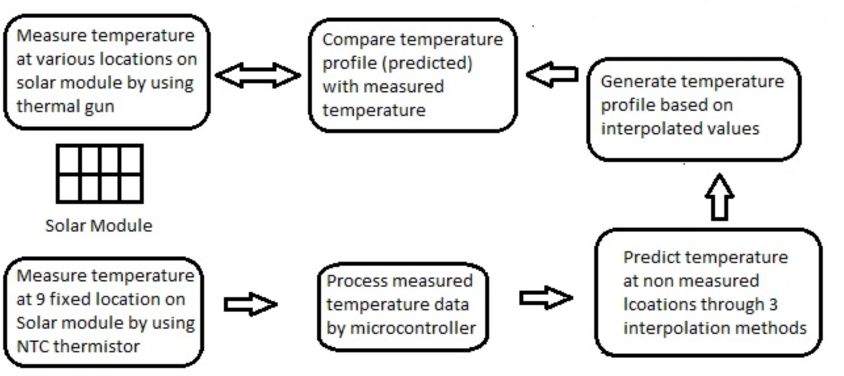

Fig. 5 Block diagram of monitoring and visualization of solar PV thermal flow

3.1 Solar Module

Solar module utilized in the project is a monocrystalline type with dimensions of 1189 x 543 x 30 mm and a standard test condition of cell at above 25ºC. Solar module is integrated with thermistor temperature sensors through the microcontroller as the thermal gradient collector. The thermistor temperature sensors are pasted on the rear surface of the solar panel with applying a thermal gel to act as an interface between the heat sink (sensor) and the heat source (solar panel), to eliminate the air gaps and maximizing the heat transfer between them.

3.2 Thermal Gun

The thermal gun used is Fluke 59 mini infrared thermometer gun which has an accuracy of ± 2% of reading within a temperature range of -18 to 275℃, it is utilized to record the measurements for verification and comparison purpose. It is also used for sensors calibration by measuring sensors temperatures.

3.3 Thermal Gradient Collector

Thermal gradient collector is a means of understanding the amount of heat radiation distributed on the surface of a solar panel. Nine NTC thermistor temperature sensors are attached to the back surface of the solar module, arranged as 3x3 (3 columns and 3 rows thermistor arrangements), all are pasted at approximately 170 mm row distance to each other and 370 mm column distance to each other as shown in Fig. 6, while the red points shown between the sensors are marked for the purpose of determination of the interpolation points required to be measured by the thermal gun method. The thermistors used are BS25 3950 NTC thermistor (10 kΩ with precision of 1%). Temperature data collection of the module were tested under temperatures between 25 to 65℃.

3.4 Temperature and Electrical Instrument Measurement

The workflow of temperature profile visualisation system is presented in Figure 7 and the details can be obtained from Hafiz [12]. The temperature thermal data collection system comprises of an Arduino Mega 2560 circuited with nine different NTC thermistor temperature sensors. Each NTC temperature sensor is connected in series with a 10 kΩ resistor to apply the voltage divider circuit, in order to convert the reading thermal value to a voltage reference reading through A0-A8 analogue pins of Arduino Mega microcontroller. Subsequently, MATLAB reads the output voltage value from the analogue pins and convert it to a digital value, in order to calculate the resistance of the thermistor sensor using Equation (1). Thereafter, MATLAB will compute the thermistor temperature with Equation (2).

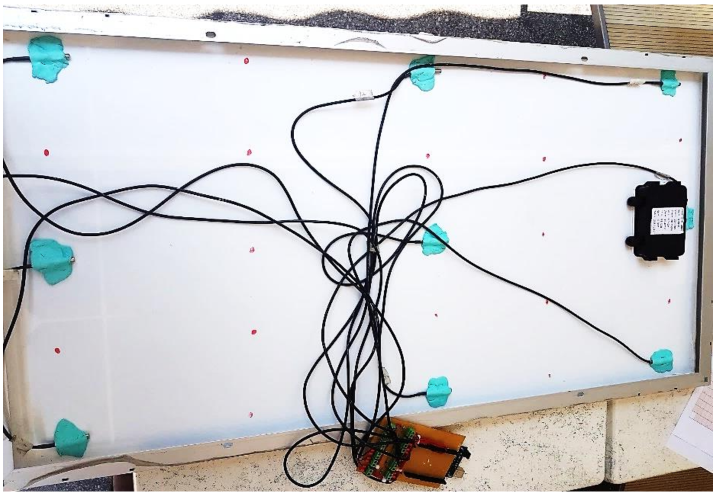

Fig. 6 Thermal gradient measurement using 3x3 NTC thermistor temperature sensors arrangement.

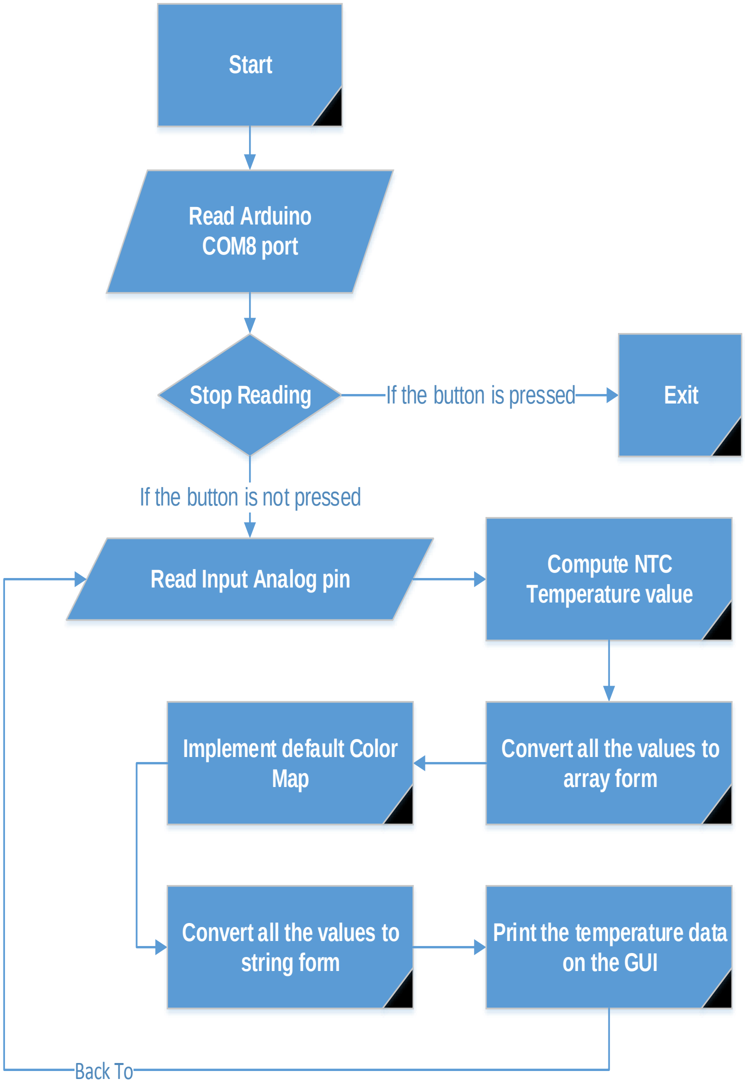

Fig. 7 Workflow of temperature profile visualisation system.

Equation (1) is derived from the voltage divider formula; while mathematical equation (2) which is known as B parameter equation, is essentially derived from Steinhart-Hart equation [13]. According to NTC thermistor linearity graph, conversion of the resistance value to absolute temperature was executed with the following equations below:

$$R = \frac{R_0}{(1023/ADC) - 1} \tag{1}$$

$$T = \frac{1}{\left[\left(\frac{1}{B_0} \times \log \frac{R}{R_0}\right) + \frac{1}{T_0}\right]} - 273.15 \tag{2}$$

Where:

B_0 = Nominal beta constant at 25 °C
R_0 = Nominal resistance at 25 °C=10kΩ
R = NTC thermistor resistance
ADC = Output voltage converted from analogue to digital signal value
1023 = 5 V input voltage equivalent in digital value
T = Thermistor temperature equation
T_0= Nominal temperature 25°C in Kelvin

3.5 Interpolation Methods of PV Module Thermal Gradient

The measured 3x3 temperature data is interpolated to 5x5 and 9x9 points for thermal image reconstruction. Three methods for data fit were used including bilinear interpolation method, cubic spline interpolation method, and nearest interpolation method.

3.5.1 Bilinear Interpolation Data Fit

Bilinear interpolation determines and displays the thermal gradient level value from a weighted average of four closest pixels to the specified input value coordinates, then it assigns this value to the output coordinates. For linear interpolation method, two grid points are required to interpolate the function for one direction interpolation problem. For two directional problem, two linear interpolations are performed continuously in two directions, which are horizontal and vertical direction as illustrated in Figure 8.

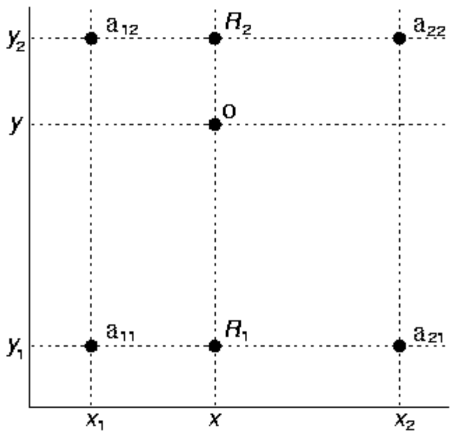

Fig. 8 Bilinear interpolation illustration.

Mathematical equations of adopted bilinear interpolation method resolved from bilinear interpolation are described as follows:

$$R_1 = \frac{(x_2 - x)}{(x_2 - x_1)} a_{11} + \frac{(x - x_1)}{(x_2 - x_1)} a_{21} \quad (3)$$

$$R_2 = \frac{(x_2 - x)}{(x_2 - x_1)} a_{12} + \frac{(x - x_1)}{(x_2 - x_1)} a_{22} \quad (4)$$

Final value "O" to calculate from R_1 and R_2 weighted average result to

$$O = \frac{(y_2 - y)}{(y_2 - y_1)} R_1 + \frac{(y - y_1)}{(y_2 - y_1)} R_2 \quad (5)$$

Where:

a_{11}, a_{12}, a_{21} and a_{22} are nearest pixel from the original image value
R_1 = weighted average from point (a_{11}) and (a_{21})
R_2 = weighted average from point (a_{12}) and (a_{22})
O = weighted average from R_1 and R_2

3.5.2 Cubic-Spline Interpolation Data Fit

The cubic spline is a piecewise polynomial interpolation scheme that can overcome the problem of polynomial wiggle in linear fit. To construct a cubic function between data points [14].

$$S_k(x) = S_{k,0} + S_{k,1}(x - x_k) + S_{k,2}(x - x_k)^2 + S_{k,3}(x - x_k)^3$$

Where $x \in [x_k, x_{k+1}]$ and the coefficient $S_{k,j}$ are to be determined from various constraint conditions. Four constraint conditions are imposed: $S_k(x_k) = y_k$

$$S_k(x_k + 1) = S_{k+1}(x_{k+1})$$

$$S_k^{'}(x_k + 1) = S_{k+1}^{'}(x_{k+1})$$

$$S_k^{''}(x_k + 1) = S_{k+1}^{''}(x_{k+1})$$

The equations are then solved with spline toolbox in MATLAB.

3.5.3 Nearest Interpolation Data Fit

For each one-dimension interpolation of original temperature sensor 3x3 data array arrangement, four closest grid points are used to evaluate each data prediction or interpolation, that is two grid points from side by side put under consideration.

4.0 RESULTS AND DISCUSSION

The interpolation temperature results from three interpolation methods (bilinear, cubic spline, and nearest) were compared with the measured temperature results from thermal gun. Five sets of temperature data were collected with thermal gun for verification. In addition, the thermal gradient images are presented in different resolution (17 x17 and 33 x 33). Solar module temperature was manually measured with a thermal gun based on 5x5, and 9x9 scaling. Fig. 9 is a 3x3 sensors arrangement, shows measured values of nine thermistor without any interpolation technique used, while Figs 10 to 12 are samples results of 17x17 interpolation scaling size and Figs 13 to 15 are samples results of 33x33 interpolation scaling size. Obviously, the images with 33x33 interpolation scaling size have better resolution compared to 17x17 interpolation scaling sizes. In addition, the nearest interpolation method is unable to provide a smooth transition in thermal gradient images (Figs 12 and 15).

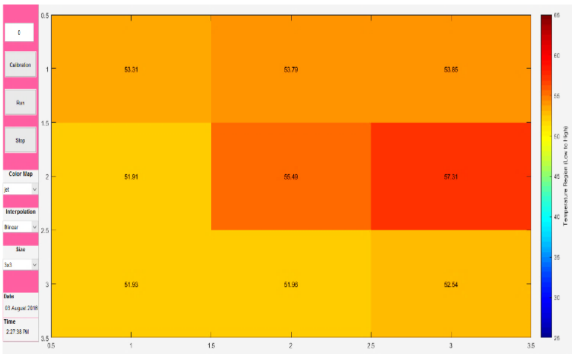

Fig. 9 Sample result of 3x3 sensors arrangement temperature readings from solar panel surface.

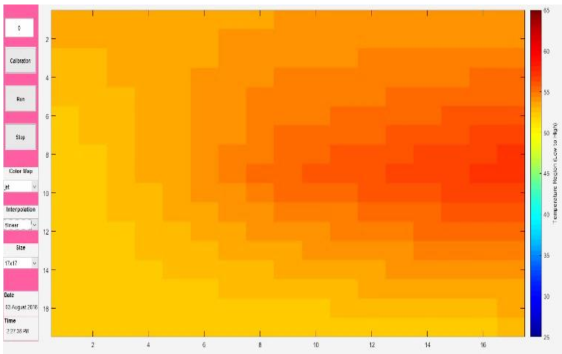

Fig. 10 Sample result of thermal gradient image reconstruction with 17x17 bilinear interpolation.

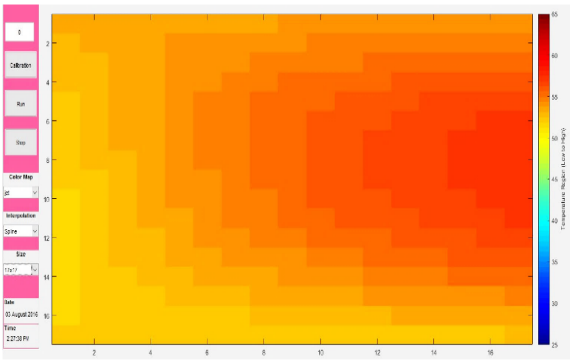

Fig. 11 Sample result of thermal gradient image reconstruction with 17x17 spline interpolation.

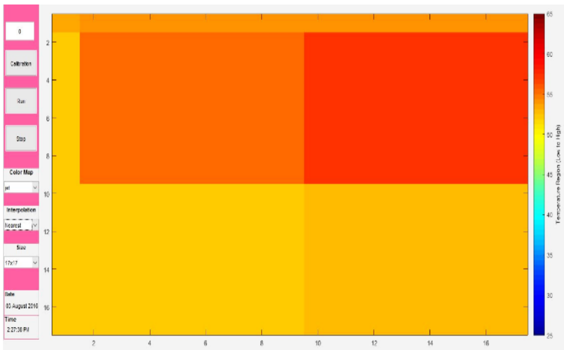

Fig. 12 Sample result of thermal gradient image reconstruction with 17x17 nearest interpolation.

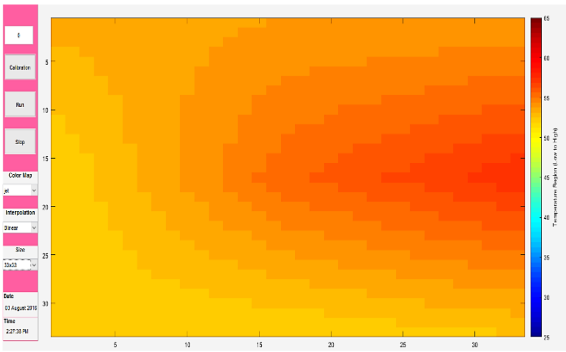

Fig. 13 Sample result of thermal gradient image reconstruction with 33x33 bilinear interpolation.

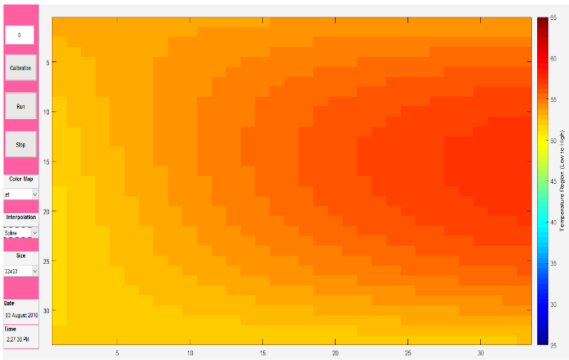

Fig. 14 Sample result of thermal gradient image reconstruction with 33x33 spline interpolation.

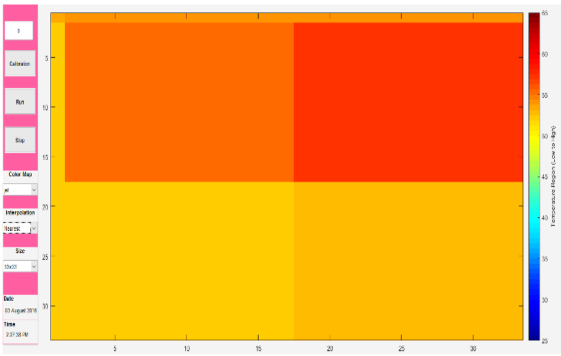

Fig. 15 Sample result of thermal gradient image reconstruction with 33x33 nearest interpolation.

The average interpolated temperature for 5 points in a column is compared with the measured temperature from thermal gun, in 5 x 5 scaling and 9 x 9 scaling, as shown in Figs 16-17. In general, bilinear interpolation method performs better than cubic spline and nearest interpolation methods for both 5 x5 and 9 x9 scaling. This is further confirmed with the approximate error of each interpolation technique as shown in Tables 1 to 2. The percent error is defined as the different between interpolated data and measured data and then divided by measured data. Comparison of the temperatures for the bilinear interpolated method and infrared thermometer method gives an average error of below 1% for both 5x5 scaling and 9x9 scaling. Fig. 12 and Fig. 15 show that nearest interpolation would be used to obtain a main overview of the major temperatures on the solar panel surface, as it essentially imitates the nearest existing sensor value to an interpolated value. On the other hand, the thermal flow predicted by bilinear (Fig. 13) and spline methods (Fig. 14) shows a difference between these two techniques in terms of heat distribution. Bilinear method shows a typical linear shape in two-dimensional space, while spline technique shows a curved shape. The different in three interpolation method is more obvious in higher resolution result (33 x 33).

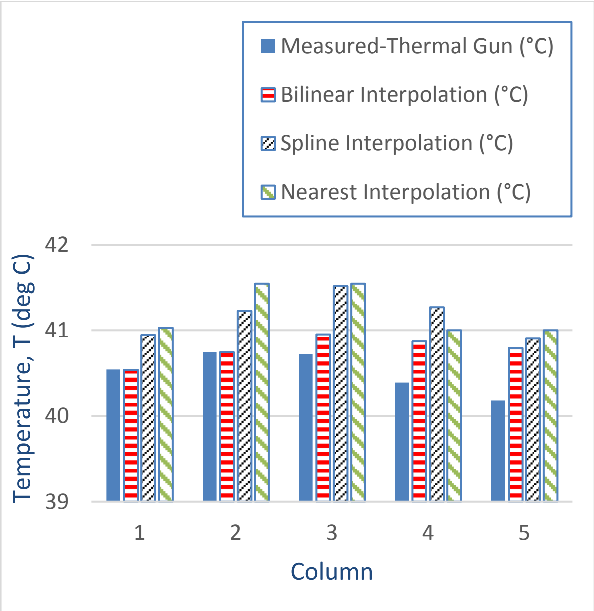

Fig. 16 Comparative bars of 5x5 temperature measurements of solar module.

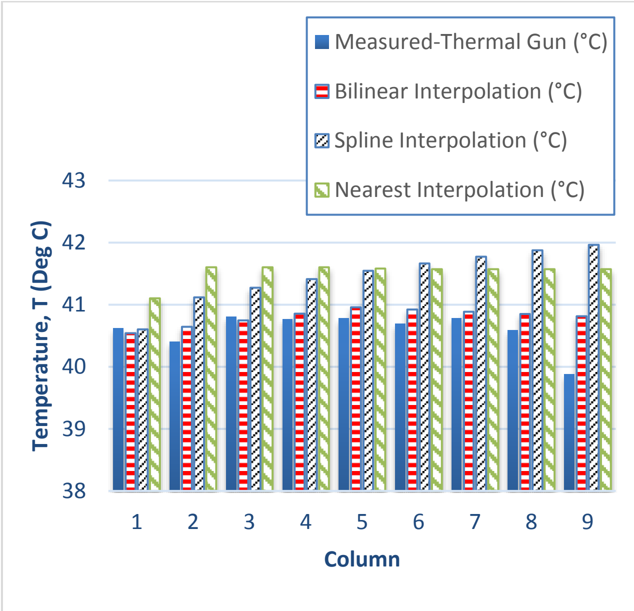

Fig. 17 Comparative bars of 9x9 temperature measurements of solar module.

Table 1. 5x5 Approximate Error Calculations

Interpolation Technique	Approximate Error (%)					Average Error (%)
Bilinear Interpolation	0.012	0.007	0.559	1.191	1.530	**0.660**
Spline Interpolation	0.987	1.181	1.949	2.176	1.805	**1.619**
Nearest Interpolation	1.198	1.961	2.021	1.504	2.040	**1.745**

Table 2. 9x9 Approximate Error Calculations

Interpolation Technique	Approximate Error (%)								Average Error (%)
Bilinear Interpolation	0.193	0.588	0.141	0.214	0.439	0.562	0.259	0.635	**0.598**
Spline Interpolation	0.039	1.763	1.139	1.586	1.875	2.388	2.440	3.162	**2.181**
Nearest Interpolation	1.194	2.961	1.952	2.052	1.963	2.161	1.944	2.419	**2.323**

5.0 CONCLUSION

Thermal profile of solar PV system is succussfuly generated with minimum temperature measurement. Temperature at nine locations on PV panel were measured by NTC thermistor. Three interpolation techniques, bilinear, cubic spline and nearest were used to estimate temperature data at 25 (5 x 5) and 81 (9 x9) strategy points based on the nine measured temperature. The bilinear method outperformed other methods in this study. The predicted temperature was then used to construct the thermal flow image of PV solar module at different resolution, 17 x17 and 33 x 33. The different among bilinear and cubic spline is more obvious at high resolution of 33 x 33. Bilinear method with resolution of 33x33 is recommended to generate thermal profile with minimum measurement points.

Acknowledgements

This project has been implemented in collaboration between UCSI University and Heriot-Watt University. Mr Choo Seng Kee and Mr Yazeed Fares Nasrallah are acknowledged for their help and support.

References

[1] Ogbomo, O.O., E. H. Amalu, N.N. Ekere, P.O. Olagbegi. 2017. A review of photovoltaic module technologies for increased performance in tropical climate. *Renewable and Sustainable Energy Reviews*. 75: 1225-1238.

[2] Belkaid, A., J. Gaubert, A. Gherbi and L. Rahmani. 2014. Maximum Power Point tracking for photovoltaic systems with boost converter sliding mode control. *2014 IEEE 23rd International Symposium on Industrial Electronics (ISIE)*, Istanbul, 556-561.

[3] Peled, A., and J. Appelbaum. 2017. Enhancing the power output of PV modules by considering the view factor to sky effect and rearranging the interconnections of solar cells. *Prog. Photovolt: Res. Appl.*, 25: 810–818.

[4] Villalva, M. G., J. R. Gazoli, and E. R. Filho. 2009. Comprehensive Approach to Modeling and Simulation of Photovoltaic Arrays. *Power Electronics, IEEE Transactions on*, 24(5): 1198–1208.

[5] ALQahtani, A. H., M. S. Abuhamdeh, and Y. M. Alsmadi. 2012. A simplified and comprehensive approach to characterize photovoltaic system performance. *2012 IEEE Energytech*, 43210(1): 1–6.

[6] Khan, M., M. Z. Khan, M. N. Imtiaz Khan, S. S. Saha, D. F. Noor, and M. R. K. Rach 2014. Maximum Power Point Tracking for Photovoltaic Array Using Parabolic Interpolation. *International Journal of Information and Electronics Engineering*, 4(3):249-255.

[7] Jones A. D. and C. P. Underwoord. 2001. A thermal model for photovoltaic systems. Solar Energy, 70(4): 349–359.

[8] King, D. L., Kratochvil, J. A. and Boyson, W. E. 2004. Photovoltaic array performance model. United States. doi:10.2172/919131.

[9] Marion, B., S. Rummel and A. Anderberg 2004. Current-voltage curve translation by bilinear interpolation. *Progress in Photovoltaics: Research and Applications*, 12(8): 593–607.

[10] Ishaque, K., Z. Salam, M. Amjad, and S. Mekhilef. 2012. An Improved Particle Swarm Optimization (PSO)-based MPPT for PV with reduced steady-state oscillation. *IEEE Transactions on Power Electronics*, 27(8): 3627–3638.

[11] Mangeni G., R.H.G. Tan, T.H. Tan, S.K. Cheo, V.H. Mok, J.Y. Pang. 2017. Photovoltaic Module Cell Temperature Measurements using Linear Interpolation Technique, *2017 IEEE International Instrumentation and Measurement Technology Conference (I2MTC)* [7969759].

[12] Hafiz, F.A. 2017. Monitoring and Visualization of Solar PV Thermal Flow via Interpolation Techniques. MSc disseratation. Heriot-Watt University. Putrajaya.

[13] Steinhart J.S. and S.R. Hart. 1968. Calibration curves for thermistors, Deep Sea Research and Oceanographic Abstracts 1968;15(4): 497-503.

[14] Kutz, J.N. 2013. Data-Driven Modeling & Scientific Computation: Methods for Complex Systems & Big Data, OUP Oxford.